JACS
JOURNAL OF THE AMERICAN CHEMICAL SOCIETY
Article
pubs.acs.org/JACS

Stacking Interactions Drive Selective Self-Assembly and Self-Sorting of Pyrene-Based $M^{II}_4L_6$ Architectures

Tanya K. Ronson, Derrick A. Roberts, Samuel P. Black, and Jonathan R. Nitschke*

Department of Chemistry, University of Cambridge, Lensfield Road, Cambridge, CB2 1EW, U.K.

Supporting Information

ABSTRACT: Subcomponent self-assembly of two isomeric bis(3-aminophenyl)pyrenes, 2-formylpyridine and the metal ions Fe^{II}, Co^{II}, and Zn^{II} led to the formation of two previously unidentified structure types: a C_2-symmetric $M^{II}_4L_6$ assembly with meridionally coordinated metal centers, and a C_3-symmetric self-included $M^{II}_4L_6$ assembly with facially coordinated metal centers. In both structures the *meta* linkages within the ligands facilitate π-stacking between the pyrene panels of the ligands. A C_{2h}-symmetric $M^{II}_2L_2$ box was also obtained, which was observed to selectively bind electron-deficient aromatic guests between two parallel pyrene subunits. Similar donor−acceptor interactions drove the selective self-assembly of a singular $M^{II}_4L_4L'_2$ architecture incorporating both a pyrene-containing diamine and an electron-deficient NDI-based diamine. This heteroleptic architecture was shown to be thermodynamically favored over the corresponding homoleptic $M^{II}_4L_6$ and $M^{II}_4L'_6$ complexes, which were nonetheless stable in each others' absence. By contrast, an isomeric pyrene-based diamine was observed to undergo narcissistic self-sorting in the presence of the NDI-based diamine.

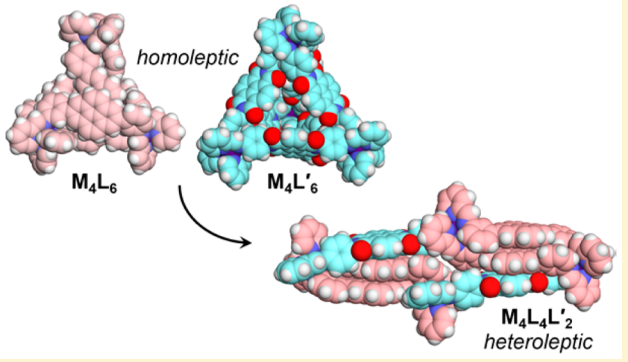

INTRODUCTION

The synthesis of new metal−organic architectures[1] has received attention due to their applications in molecular recognition,[2] separations,[3] reactivity modulation[4] and catalysis[5] and as part of a broader interest in the design of complex self-assembled structures from simple components.[1b] Knowledge of geometrical principles and the stereoelectronic preferences of metal ions combined with the use of rigid multidentate ligands has led to the rational design[6] of a diverse range of highly symmetric[7] polyhedral architectures including tetrahedra,[8] cubes,[9] octahedra,[10] dodecahedra[11] and spheres.[12] However, the relationship between the chemical structure of a supramolecular building block and the three-dimensional architecture into which it self-assembles is not well established, and even relatively simple self-assembly reactions that employ only a single ligand type (i.e., homoleptic) frequently have outcomes guided more by serendipity than design.[13]

Functional structures in biological systems are often assembled from many different building blocks in a precise geometric arrangement;[14] mimicking this route to structural complexity in synthetic systems offers a means of achieving the more sophisticated functions associated with structural complexity. One approach to increasing the intricacy of self-assembled architectures is to increase the number of distinct components that comprise them.[15] Heteroleptic self-assembly (i.e., employing more than one type of ligand) has been shown to produce unusual and complex supramolecular architectures that often exhibit lower symmetries than their homoleptic counterparts.[16] Such heteroleptic metal−organic assemblies[17] frequently incorporate ligands with different donor atoms,[18] although examples incorporating ligands with similar coordinative environments[19] are also known. The rational design of such architectures remains challenging and new reports of complex heteroleptic assemblies will be crucial for elucidating the design principles[17,20] behind their construction.

Although the formation of metal−ligand bonds often provides the predominant means of defining the structures of self-assembled metal−organic architectures, other factors, such as steric hindrance[21] and templation by ionic[22] or neutral guests,[23] can also influence the outcome of self-assembly processes. Electrostatic interactions between electron-rich and electron-poor aromatics provide an important driving force in the self-assembly of foldamers,[24] rotaxanes,[25] catenanes,[26] inclusion complexes[27] and polymers.[28] We have recently demonstrated that such donor−acceptor interactions can be used to prepare a dynamic combinatorial library (DCL) of polycatenated tetrahedra from a dynamic Fe_4L_6 tetrahedral cage containing electron-deficient naphthalenediimide (NDI) based ligands.[29] Aromatic stacking interactions between electron-poor and electron-rich ligand fragments have also been shown to contribute substantially to the stability of pyridyl-pyrazole based coordination cages,[9a] suggesting that the influence of such π-

Received: September 21, 2015
Published: October 28, 2015

DOI: 10.1021/jacs.5b09920
J. Am. Chem. Soc. 2015, 137, 14502−14512

Scheme 1. Subcomponent Self-Assembly of Homeleptic and Heteroleptic Metal-Organic Assemblies from Diamines A–C[a]

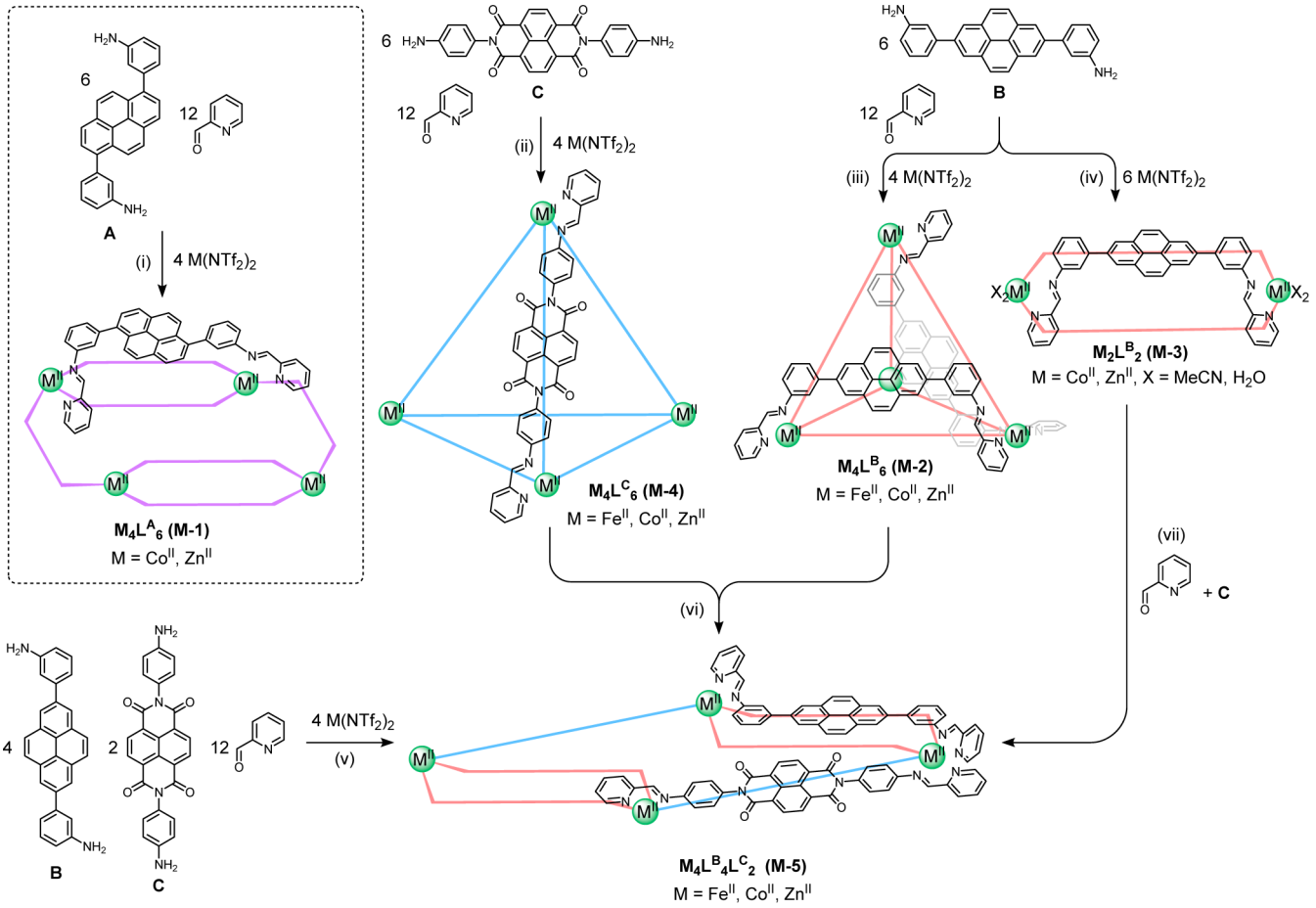

[a](i) Preparation of M-**1** (M = Co^{II}, Zn^{II}) from $M(NTf_2)_2$, 1,6-bis(3-aminophenyl)pyrene (**A**) and 2-formylpyridine in a 2:3:6 ratio. (ii) Preparation of M-**3** (M = Fe^{II}, Co^{II}, Zn^{II}) from $M(NTf_2)_2$, NDI-based diamine (**C**) and 2-formylpyridine in a 2:3:6 ratio. (iii, iv) Preparation of M-**2** (M = Fe^{II}, Co^{II}, Zn^{II}) and M-**3** (M = Co^{II}, Zn^{II}) from $M(NTf_2)_2$, 2,7-bis(3-aminophenyl)pyrene (**B**) and 2-formylpyridine in a 2:3:6 ratio or 1:1:2 ratio, respectively. (v–vii) Preparation of heteroleptic assembly M-**5** (M = Fe^{II}, Co^{II}, Zn^{II}) through three alternative routes: (v) subcomponent self-assembly of $M(NTf_2)_2$, **B**, **C** and 2-formylpyridine in a 2:2:1:6 ratio, (vi) reaction of homoleptic assemblies M-**2** and M-**4** in 2:1 ratio, or (vii) addition of **C** (1 equiv) and 2-formylpyridine (2 equiv) to M-**3**. All reactions were carried out in acetonitrile. One or two ligands are shown in the schematic representations for clarity, with additional ligands being represented as lines between the metal centers (shown as green spheres).

stacking interactions[30] on the assembly of metal–organic architectures bears wider exploration.

Subcomponent self-assembly[31] has been demonstrated to be a versatile approach for the construction of increasingly complex metallosupramolecular architectures. In many cases, small changes to the structure of a subcomponent can produce major changes in the architecture and recognition properties[23b,32] of the resulting assemblies. Herein we demonstrate the preparation of two structurally distinct nontetrahedral $M^{II}_4L_6$ assemblies from two isomeric pyrene-containing diamines. *Meta*-substituted anilines were chosen to bring the ligand arms close enough to undergo π-stacking, in contrast to previously reported $M^{II}_4L_6$ cages prepared from analogous *para*-substituted anilines, for which no such interactions were observed.[32] Furthermore, we show that favorable pyrene-NDI π-stacking interactions can be used to direct the self-assembly of a unique triple-decker heteroleptic $M^{II}_4L_4L'_2$ sandwich complex.

RESULTS AND DISCUSSION

Self-Assembly of Homoleptic $M^{II}_4L_6$ Architectures. Bis(3-aminophenyl)pyrene derivatives **A** and **B** (Scheme 1) were each prepared in a single step from commercially available starting materials via Pd-catalyzed Suzuki–Miyaura cross-coupling reactions[33] (synthetic details are provided in the Supporting Information). The ligands derived from the condensation of diamines **A** and **B** with 2-formylpyridine (L^A and L^B respectively) possess offset coordination vectors, which may be arranged in different orientations, rendering the outcome of their self-assembly with octahedral metal ions difficult to predict through established rational design principles.

The reaction of diamine **A** (6 equiv) with 2-formylpyridine (12 equiv) and zinc(II) bis(trifluoromethane)sulfonimide ($Zn(NTf_2)_2$, 4 equiv) in CH_3CN at 323 K yielded a new product Zn-**1** (Scheme 1, (i)) with a well-resolved but complicated ^{1}H NMR spectrum. All peaks between 4.9 and 9.7 ppm displayed a single diffusion constant in the diffusion ordered ^{1}H NMR (DOSY) spectrum, suggesting that they belonged to a single species. One-dimensional pure shift (PSYCHE)[34] and two-dimensional NMR spectroscopy allowed the assignment of the major peaks to six magnetically distinct environments of equal intensity per ligand proton, consistent with the formation of a product of C_2 symmetry. Electrospray

DOI: 10.1021/jacs.5b09920
J. Am. Chem. Soc. 2015, 137, 14502–14512

ionization mass spectrometry (ESI-MS) of Zn-**1** was consistent with the formulation $Zn^{II}_4L_6$.

The solid-state structure of Zn-**1** was elucidated by single-crystal X-ray analysis. The crystal structure revealed a $Zn^{II}_4L_6$ assembly composed of four meridionally coordinated octahedral zinc centers bridged by six bis(pyridylimine)ligands (Figure 1). The complex can be regarded as being composed

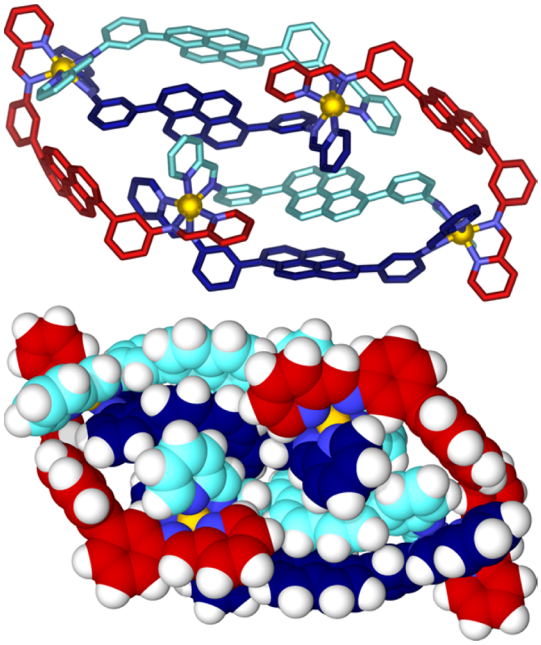

Figure 1. Two views of the cationic part of the crystal structure of Zn-**1** with neighboring ligands colored differently for contrast. Counterions, solvents and disorder are omitted for clarity.

of two double helical $Zn^{II}_2L_2$ units (Zn−Zn separations 17.2−17.4 Å) further linked together by two axial ligands (Zn−Zn separations 11.5−11.9 Å). The four zinc centers in Zn-**1** are roughly coplanar, and form a rhomboid with the complex possessing approximate C_2 point symmetry. The structure is stabilized by face-to-face π-stacking interactions between the two pyrene backbones of each Zn_2L_2 helicate and numerous CH-π interactions. The meridional coordination in Zn-**1** differs from the facial coordination observed in the majority of M_4L_6 assemblies which typically display a (pseudo)tetrahedral array of metal centers; rare examples of such assemblies with one *fac* center and three *mer* centers[35] or four *mer* centers[36] have also been reported.

The solid state structure of Zn-**1** is consistent with the NMR and ESI-MS data obtained from solution-based studies. The two distinct types of *mer* center in the structure are consistent with the six nonequivalent NMR environments observed in the ^{1}H NMR spectrum of Zn-**1**. Several proton resonances, including one imine signal at 4.97 ppm, appear significantly upfield-shifted as a result of CH-π interactions with the pyrene units. Minor peaks were observed in the ^{1}H NMR spectrum of Zn-**1**, corresponding to less than 10% of the total integrated intensity, which we infer to correspond to other isomers. The assembly of Zn-**1** is thus not perfectly selective, although more than 90% so.

Similarly, the reaction of **A** (6 equiv) with 2-formylpyridine (12 equiv) and $Co(NTf_2)_2$ (4 equiv) at 323 K in CH_3CN yielded a $Co^{II}_4L_6$ assembly as confirmed by ESI-MS. The ^{1}H NMR spectrum also revealed six magnetically distinct environments per ligand proton, with the signals spread over the range −36 to +273 ppm as a result of the paramagnetism of Co^{II}. Single-crystal X-ray analysis of the product Co-**1** confirmed it to be isostructural with Zn-**1**. By contrast, when $Fe(NTf_2)_2$ was employed in the self-assembly reaction a broad and intractably complicated ^{1}H NMR spectrum was observed, inconsistent with the formation of a single well-defined species in solution. No further changes to the NMR spectrum were observed upon heating the mixture to 353 K for 7 days. We infer the slightly distorted octahedral geometry present in the structures of Zn-**1** and Co-**1** to be incompatible with the rigid geometrical requirements imposed by low-spin iron(II).[22a,37]

The reaction of diamine **B** (6 equiv) with 2-formylpyridine (12 equiv) and $Zn(NTf_2)_2$ (4 equiv) in CH_3CN at 323 K yielded a new product Zn-**2** (Scheme 1, (iii)), which was also confirmed to have $Zn^{II}_4L_6$ stoichiometry by ESI-MS. The ^{1}H NMR spectrum of Zn-**2** was sharp and well resolved; two-dimensional NMR spectroscopy allowed the assignment of the major set of peaks to four distinct ligand environments. The DOSY spectrum was consistent with the presence of a single species in solution. Similarly, the reaction of **B** (6 equiv) with 2-formylpyridine (12 equiv) and $Fe(NTf_2)_2$ or $Co(NTf_2)_2$ (4 equiv) in CD_3CN yielded $M^{II}_4L_6$ assemblies Fe-**2** and Co-**2**, as confirmed by ESI-MS. When these reactions were carried out at 323 K, the ^{1}H NMR spectra of the reaction mixtures showed multiple broad peaks suggesting the presence of complex mixtures of species; however, subsequent heating at 353 K for 24 h led to the formation of products displaying sharp, well-resolved spectra consistent with the presence of a single product with four magnetically distinct environments per ligand proton.

Vapor diffusion of benzene into an acetonitrile solution of Fe-**2** afforded crystals suitable for single-crystal X-ray diffraction analysis. Two representations of the X-ray structure of Fe-**2** are shown in Figure 2. The structure consists of four facially coordinated octahedral iron(II) centers in a pseudotetrahedral arrangement linked by six bis-bidentate ligands. The complex displays two distinct ligand configurations: Three basal ligands are arranged on the outside of the structure, bridging between pairs of iron(II) centers around the bottom face of the pseudotetrahedron (Fe−Fe distances 16.2−16.6 Å). Three axial ligands occupy the interior of the structure, each linking the apical iron(II) center with one of the basal iron(II) centers (Fe−Fe distances 16.6−17.5 Å). The pyrene backbone of each axial ligand undergoes face-to-face π-stacking with the pyrene moiety of a basal ligand, with pyrene−pyrene distances of 3.4−3.6 Å; the three pairs of π-stacked pyrenes completely occupy the tetrahedral cavity, eliminating any possible internal void space. The interior pyrenes also undergo edge-to-face stacking with each other, with CH-pyrene separations of 2.54−2.81 Å. All four iron(II) centers within a single assembly display the same Δ or Λ chirality; both enantiomers of Fe-**2** are present in the unit cell, related through inversion symmetry. The structure displays noncrystallographic C_3 symmetry, with a 3-fold symmetry axis passing through the center of the basal face (Figure 2). The nature of the C_3 symmetry observed in Fe-**2** is distinct from that observed in previously described C_3-symmetric M_4L_6 cages, which possess a ΔΔΔΛ or ΛΛΛΔ arrangement of metal centers.[32,38]

The solution NMR data for assemblies M-**2** (M = Fe^{II}, Co^{II}, Zn^{II}) are all consistent with the solid state structure of Fe-**2**, with the basal metal centers giving rise to three distinct

DOI: 10.1021/jacs.5b09920
J. Am. Chem. Soc. 2015, 137, 14502−14512

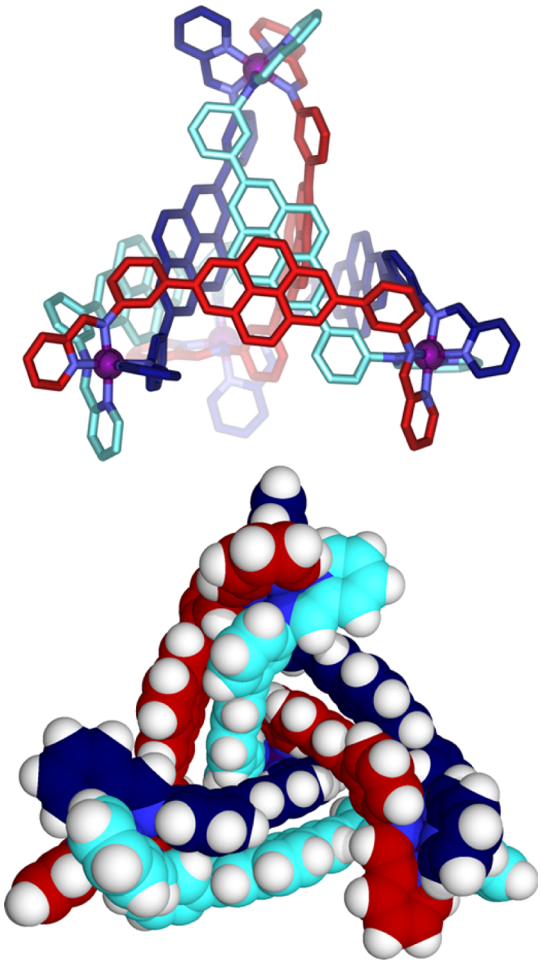

Figure 2. Two views of the cationic part of the crystal structure of Fe-**2** with neighboring ligands colored differently for contrast. Counterions, solvents and disorder are omitted for clarity.

magnetic environments and the apical metal center giving rise to one environment. The highly upfield-shifted pyrene resonances observed at 4.22 and 2.16 ppm in the ^{1}H NMR spectra of Fe-**2** and at 4.12 and 2.13 ppm in the ^{1}H NMR spectra of Zn-**2** are consistent with the π-stacking observed in the solid state (SI, Section S3.3.1). Similarly, the ^{1}H NMR spectrum of Co-**2** shows paramagnetically shifted resonances out to −81.4 ppm, consistent with those observed for other cobalt(II) based assemblies containing substantial aromatic stacking interactions.[2b]

All 52 proton environments in the ^{1}H NMR spectrum of Fe-**2** were assigned using a combination of selective 1D TOCSY, NOESY and ROESY techniques. Selective 1D TOCSY (SI, Figures S26−S30) clearly highlighted the four sets of pyridyl- and aniline-derived spin systems. Unexpectedly, 1D selective NOESY and ROESY measurements revealed the outer pyrene rings of Fe-**2** to rotate slowly on the NMR time scale, indicating that the complex is remarkably flexible despite the close contacts between pyrene subunits observed in the crystal structure. 1D selective EXSY NMR revealed the approximate rate of rotation to be 0.18 ± 0.04 s^{-1} at 298 K, approximately one rotation every 4−6 s (SI, Section S3.3.2). The dynamic behavior of Fe-**2**, despite the apparent internal steric hindrance, has more general implications in the context of how supramolecular hosts might distort to allow the passage of large guests through small pores in their frameworks.[39]

When a mixture of the two diamines **A** (3 equiv) and **B** (3 equiv), 2-formylpyridine (12 equiv) and $Zn(NTf_2)_2$ (4 equiv) in CD_3CN was heated to 323 K, a clean mixture of the homoleptic assemblies Zn-**1** and Zn-**2** was observed after 24 h, as confirmed by ^{1}H NMR (Scheme 2, Figure S86). We infer the

Scheme 2. Synthesis of Zn-1 and Zn-2 through Narcissistic Self-Sorting

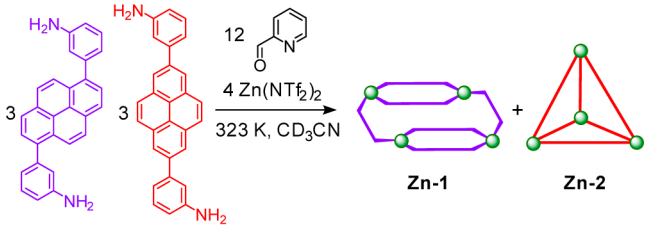

narcissistic self-sorting[40] of the *fac*- and *mer*-based assemblies to be due to geometrical differences imposed by the metal-centered stereochemistry in the two assemblies, as well as favorable π-stacking within each individual assembly.

Self-Assembly and Guest-Binding Properties of a M_2L_2 Box. The reaction of diamine **B** with 2-formylpyridine and $Zn(NTf_2)_2$ in a 1:2:1 ratio gave rise to a unique product, Zn-**3** (Scheme 1, (ii)). In contrast to the complicated ^{1}H NMR spectrum of Zn-**2**, the new product showed a single major set of resonances for each ligand proton. ESI-MS was consistent with formation of a $Zn^{II}_2L_2$ assembly. Under the same conditions $Co(NTf_2)_2$ also gave rise to a $Co^{II}_2L_2$ assembly, although the ^{1}H NMR spectrum was significantly broadened in comparison with that of Co-**2**. However, when $Fe(NTf_2)_2$ was employed under analogous circumstances, only peaks corresponding to Fe-**2** could be identified in the ^{1}H NMR and ESI-MS spectra, indicating the high stability of Fe-**2** relative to a putative Fe_2L_2 assembly, which could not satisfy the preference of iron(II) for a *tris*(pyridylimine) coordination sphere.

Single crystal X-ray diffraction revealed the structure of Zn-**3** to be a box-like achiral complex, or "mesocate"[41] of approximate C_{2h} symmetry, in which each of the two ligands bridges metal ions of opposite handedness, rather than linking between metal ions of identical handedness (Figure 3a). Each octahedral zinc(II) center is coordinated by a bidentate pyridylimine arm from each ligand, with the remaining two coordination sites occupied by acetonitrile solvent molecules. The two zinc(II) centers are separated by 18.6375(9) Å; the ligand thus adopts a more extended configuration in Zn-**3** than in Fe-**2**. The two pyrene units are arranged in a parallel-offset orientation with respect to each other, separated by a distance of 6.72 Å, which precludes any aromatic stacking interactions. Single-crystal X-ray analysis of Co-**3** (Figure S105) confirmed it to be isostructural and isomorphous with Zn-**3**.

The pyrene−pyrene separation in Zn-**3** prompted us to explore the possibility of intercalating planar aromatic guest molecules into Zn-**3**. The molecules shown in Figure 4 were screened as potential guests. Zn-**3** was initially investigated as a host for the polycyclic aromatic hydrocarbons coronene, perylene, pyrene, triphenylene and napthalene. In all cases the ^{1}H NMR signals for Zn-**3** appeared at the same chemical shifts (±0.03 ppm) as in the absence of the prospective guest, and the signals for the prospective guest were identical to those in the absence of host, suggesting that these molecules are not

DOI: 10.1021/jacs.5b09920
J. Am. Chem. Soc. 2015, 137, 14502−14512

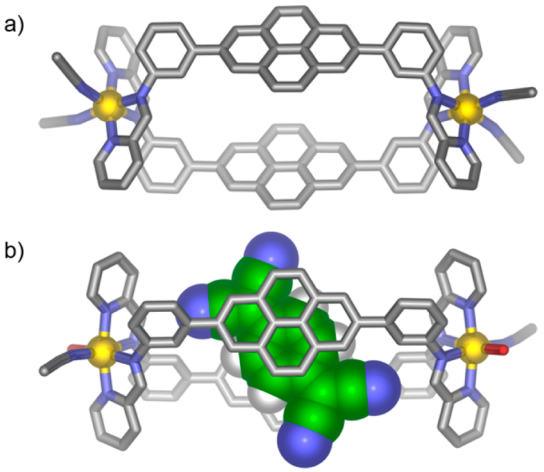

Figure 3. (a) The crystal structure of Zn-**3**. (b) The crystal structure of TCNQ⊂Zn-**3** with the TCNQ guest shown in space-filling mode. Counterions, solvents and disorder are omitted for clarity.

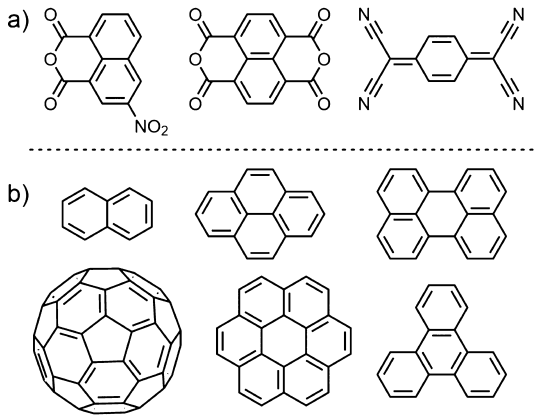

Figure 4. (a) Guests for Zn-**3** which showed fast-exchange binding by NMR; (b) compounds for which no evidence was observed for encapsulation within Zn-**3**.

encapsulated by Zn-**3**. Next, we investigated Zn-**3** as a host for the electron-poor aromatic molecules 1,4,5,8-naphthalene tetracarboxylic dianhydride, tetracyanoquinodimethane (TCNQ) and 3-nitro-1,8-naphthalic anhydride. In all cases shifts in signals of the ^{1}H NMR spectra of both host and guest were observed, consistent with fast-exchange host occupation on the ^{1}H NMR time scale.

The binding of TCNQ was also confirmed in the solid state through single-crystal X-ray diffraction analysis (Figure 3b). The structure of TCNQ⊂Zn-**3** confirms that a single molecule of TCNQ intercalates within Zn-**3**, undergoing aromatic stacking interactions between the pyrene units, with an average distance of 3.41 Å separating the stacked rings, similar to the distance of 3.38 Å observed in the structure of pyrene-TCNQ.[42] The octahedral coordination sphere of each zinc(II) center is completed by one acetonitrile and one water molecule.

No binding was observed with spherical C_{60}, indicating that Zn-**3** does not undergo any guest induced rearrangement[23a] under the experimental conditions employed.

Self-Assembly of a Heteroleptic $M_4L_4L'_2$ Architecture. The binding of electron deficient guests within mesocate Zn-**3** prompted us to explore the synthesis of heteroleptic assemblies by employing a ligand with electron deficient panels in place of the simple guests. We envisioned that favorable donor–acceptor stacking interactions[43] between the pyrene units of **B** and an electron deficient ligand may enable the self-assembly of heteroleptic metal–organic architectures that would otherwise be difficult to access through simple geometric design principles. Naphthalenediimide (NDI) based diamine **C**[44] was chosen for this purpose based on its similar size to diamine **B**. We report elsewhere the synthesis of Zn_4L_6 tetrahedral cage Zn-**4** from the subcomponent self-assembly of **C** with 2-formylpyridine and $Zn(NTf_2)_2$ (Scheme 1, (ii)).[44] Similarly, **C** was observed to form tetrahedral cages with iron(II) and cobalt(II) (see Supporting Information for further details).

The crystal structure of Co-**4** was obtained during the course of this work (Figure 5). Similarly to Zn-**4**,[44] Co-**4** crystallized as

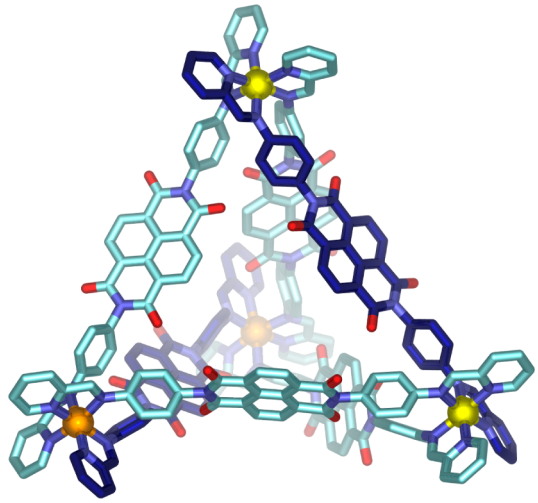

Figure 5. Crystal structure of Co-**4**, consisting of two Δ (orange) and two Λ (yellow) metal vertices, and two *anti* (dark blue) and four *syn* ligands (cyan). Anions, solvent, hydrogen atoms and disorder are omitted for clarity.

the achiral S_4 (ΛΛΔΔ) diastereomer. This diastereomer was also the predominant one observed in solution for cages M-**4** (M = Fe^{II}, Co^{II}, Zn^{II}), with small proportions of the homochiral *T* (ΔΔΔΔ/ΛΛΛΛ) and heterochiral C_3 (ΔΔΔΛ/ΛΛΛΔ) diastereomers also detected. The metal–metal separations in Co-**4** are in the range 20.5–21.0 Å, slightly longer than those observed in Fe-**2** and Zn-**3**. The NDI units in Co-**4** are too far from each other to be involved in any intramolecular face-to-face or edge-to-face π-stacking interactions.

In an initial experiment, diamine **C** (1 equiv) and additional 2-formylpyridine (2 equiv) were added to a solution of Zn-**3** (1 equiv) in CH_3CN and the mixture was maintained at 323 K for 24 h, giving rise to a clear orange solution (Scheme 1, (vii)). Examination of the ^{1}H NMR spectrum of the reaction mixture showed that the peaks for Zn-**3** had disappeared and a new set of signals was observed that did not correspond to either of the homoleptic assemblies Zn-**2** or Zn-**4**. A similar spectrum was obtained from the direct reaction of diamine **B** (4 equiv), diamine **C** (2 equiv), 2-formylpyridine (12 equiv) and $Zn(NTf_2)_2$ (4 equiv) in CH_3CN at 323 K (Scheme 1, (v)). ESI-MS of the new product Zn-**5** was consistent with the formulation $Zn^{II}{}_4L^B{}_4L^C{}_2$, where L^B and L^C are the bis-(pyridylimine) ligands derived from condensation of diamines **B** and **C** with 2-formylpyridine. Small amounts of Zn-**4** were also observed in the ESI-MS spectrum, whereas no peaks

DOI: 10.1021/jacs.5b09920
J. Am. Chem. Soc. 2015, 137, 14502–14512

corresponding to homoleptic assemblies of L^B (Zn-**2** or Zn-**3**) were detected. The reaction of $Fe(NTf_2)_2$ and $Co(NTf_2)_2$ with a mixture of diamines **B** and **C** under the same conditions also gave rise to new products with formula $M^{II}{}_4L^B{}_4L^C{}_2$ (M^{II} = Fe^{II}, Co^{II}), as indicated by ESI-MS. In each case the ^{1}H NMR spectra of the new products contained peaks that did not correspond to the homoleptic assemblies of either ligand (Figures S90 and S92).

The solid-state structure of Zn-**5** was determined by single-crystal X-ray analysis. Two representations of this structure are shown in Figure 6. The crystal structure revealed a $Zn_4L^B{}_4L^C{}_2$

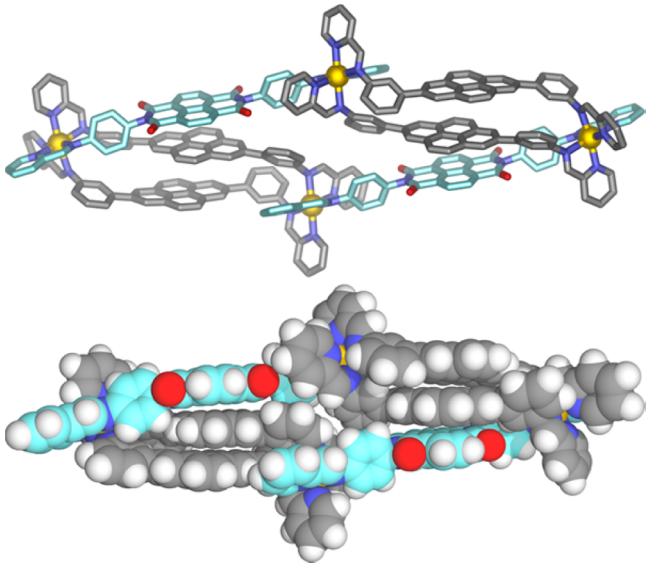

Figure 6. Two views of the crystal structure of heteroleptic assembly Zn-**5**, with the pyrene- and NDI-based ligands colored differently. Anions, solvent and disorder are omitted for clarity.

sandwich structure composed of two *fac* Zn^{II} centers, located at either end of the assembly, and two *mer* Zn^{II} centers, in the middle of the assembly. The structure of Zn-**5** is significantly elongated as compared to the assemblies obtained from each ligand individually, with a distance of 38.071(2) Å between the *fac* zinc centers at the far ends of the complex.

Each *fac* zinc center is connected to one central *mer* zinc center through two bridging pyrene-based L^B ligands (Zn−Zn distance 18.534(1) Å) and to the other *mer* zinc center by a single bridging NDI-based L^C ligand (Zn−Zn distance 20.769(2) Å), allowing the two ligands to be incorporated into the same assembly despite differences in their preferred metal−metal separations. This arrangement results in extensive π-stacking between the ligand backbones which are arranged into two pyrene−pyrene−NDI stacks with distances of ca. 3.5 Å between the mean planes of the stacked rings. The donor−donor−acceptor arrangement observed here contrasts with the complementary alternating stacks of donor and acceptor aromatic moieties that are generally regarded as the most favorable arrangement for providing optimum electronic overlap.[45] We infer that the pyrene−pyrene−NDI stacks in Zn-**5** provide the maximum face-to-face π-stacking (thus minimizing solvent-exposed surface area) while at the same time positioning the ligand arms such that the octahedral coordination preference of the metal centers can be satisfied.[25a,39] Interestingly, conversion of Zn-**3** to Zn-**5** was also observed to take place in the presence of guests such as TCNQ. Addition of diamine **C** (1 equiv) and 2-formylpyridine (2 equiv) to an acetonitrile solution of TCNQ⊂Zn-**3** thus resulted in conversion to Zn-**5** and consequent expulsion of the bound guest.

The stoichiometry of subcomponents employed is crucial to the formation of $Zn_4L^B{}_4L^C{}_2$. When a 1:1 ratio of the two ligands was employed, a complex mixture of products was obtained with little or no Zn-**5** observed by ^{1}H NMR or ESI-MS. Likewise, a 1:2 ratio of diamines **B** and **C** led to the observation of Zn-**4** as the major product in the reaction mixture. By contrast, $Fe_4L^B{}_4L^C{}_2$ formed regardless of the ratio of **B** and **C** with increasing amounts of Fe-**4** observed in addition to the heteroleptic species Fe-**5** as the proportion of **C** in the reaction mixture increased.

Further experiments were carried out to probe the stabilities of heteroleptic assemblies M-**5** relative to those of the homoleptic $M^{II}{}_4L_6$ assemblies M-**2** and M-**4**. A mixture of Zn-**2** (2 equiv) and Zn-**4** (1 equiv) was allowed to equilibrate in CD_3CN for 12 h at 323 K (Scheme 1, (vi)). Analyses of the reaction mixture by ^{1}H NMR and ESI-MS were consistent with the presence of Zn-**5** as the predominant product in solution (Figures S94 and S95). Similar results were obtained for Fe-**5** and Co-**5**, indicating that M-**5** is the thermodynamically favored product when M-**2** and M-**4** are mixed. The preferential synthesis of a single well-defined structure from a mixture of two ligands is an example of integrative self-sorting, whereby several different subcomponents are incorporated into a single architecture with precise positional control.[14,46]

Self-Sorting Experiments. In order to investigate the generality of the synthesis of heteroleptic complexes such as Zn-**5**, mixed-ligand reactions were carried out with $Zn(NTf_2)_2$, NDI-based diamine **C** and pyrene-based diamines **A**, **D** and **E** (Scheme 3).[32] The product distributions were analyzed by ^{1}H NMR and ESI-MS.

The reaction of diamines **A** (4 equiv) and **C** (2 equiv), 2-formylpyridine (12 equiv) and $Zn(NTf_2)_2$ (4 equiv) in CD_3CN at 323 K gave a clean mixture of the homoleptic assemblies Zn-**1** and Zn-**4** (Scheme 3b) as confirmed by ^{1}H NMR (Figure S76) and ESI-MS (Figure S77). We infer that the system forms, in this case, homoleptic assemblies because the mismatch of the metal−metal distances imposed by L^A and L^C precludes the formation of π-stacks, such as those observed for Zn-**5**.

By contrast, when a mixture of diamines **D** (4 equiv) and **C** (2 equiv), 2-formylpyridine (12 equiv) and $Zn(NTf_2)_2$ (4 equiv) in CD_3CN was heated to 323 K for 24 h, ESI-MS analysis of the resulting mixture showed peaks arising from all seven of the possible Zn_4L_6 assemblies, i.e., $Zn_4L^D{}_xL^C{}_{(6-x)}$ (where x = 0−6) (Scheme 3c). The distribution of species observed by ESI-MS approximates a statistical distribution, indicating that all assemblies possess similar stability. The large number of overlapping resonances rendered NMR spectroscopy unsuitable for analyzing this complex system further and the dynamic nature of the library members precluded isolation of individual species from the mixture.[29]

Similarly, a dynamic combinatorial library (DCL) of $Zn_4L^E{}_xL^C{}_{(6-x)}$ assemblies was also observed when diamine **E** was employed in the mixed-ligand self-assembly process (Scheme 3d). We infer that the use of bis(4-aminophenyl)-pyrene derivatives **D** and **E** prevents the pyrene units of the ligand from being brought into an orientation suitable for π-stacking with the NDI units of **C**; however, these ligands are

DOI: 10.1021/jacs.5b09920
J. Am. Chem. Soc. 2015, 137, 14502−14512

Scheme 3. Outcomes of Subcomponent Self-Assembly with Mixtures of Pyrene- and NDI-Based Diamines

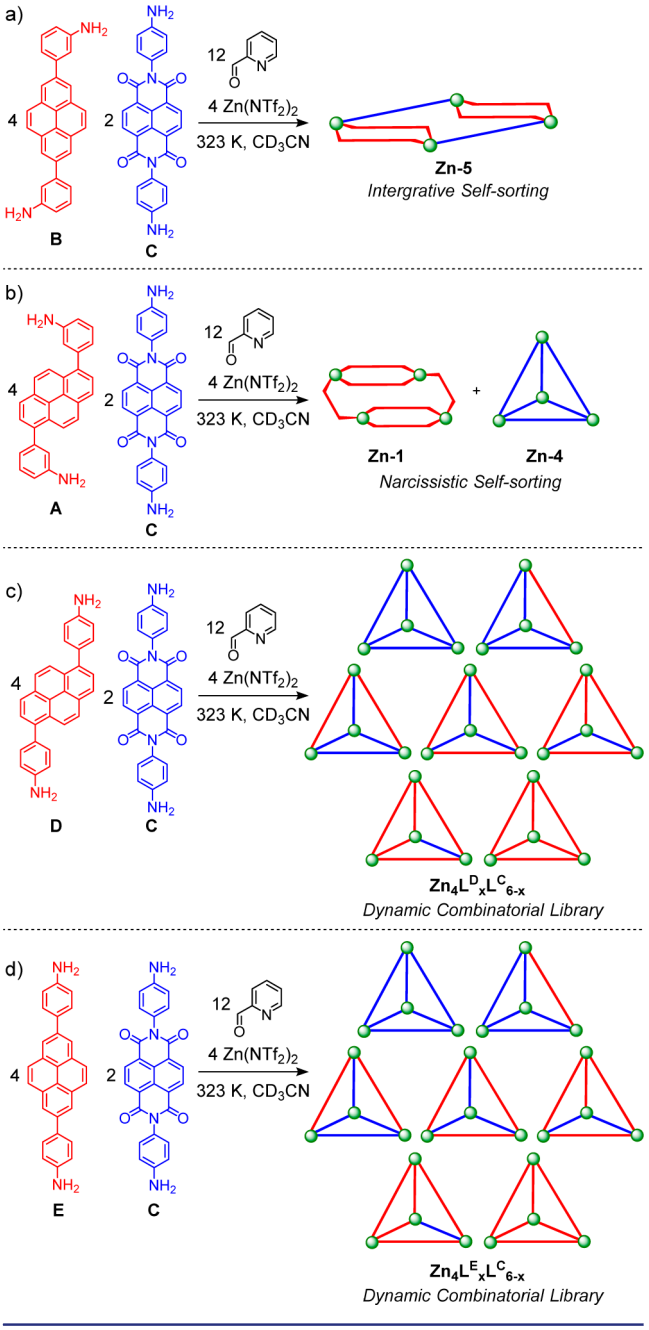

sufficiently similar in length to be incorporated into the same assembly without significant steric strain.

Finally, we probed the influence of the pyrene-NDI π-stacking as opposed to simple steric factors on the preferential self-assembly of heteroleptic structures of the type M-**5**. Pyrene-based diamine **E** was employed in place of NDI-based diamine **C** in the mixed-ligand self-assembly process; **E** has a nearly identical length and geometry to diamine **C**, differing in the more electron-rich character of its central aromatic unit. If steric factors were the dominant factor in the formation of M-**5**, we would expect diamine **E** to behave similarly to **C**. In this case, we chose to investigate the self-assembly process with iron(II), as we have previously observed diamine **E** to form a stable homoleptic M_4L_6 assembly with iron(II).[32,47] A mixture of diamines **E** (2 equiv) and **B** (4 equiv), 2-formylpyridine (12 equiv) and $Fe(NTf_2)_2$ (4 equiv) in CD_3CN was heated at 353 K for 24 h. The ^{1}H NMR spectrum of the resulting mixture was complicated, with numerous overlapping and broad resonances, inconsistent with the presence of a single assembly in solution. The ^{1}H NMR spectrum of the mixture could not be matched to a combination of the homoleptic assemblies of either ligand, indicating that a more complex mixture of species had formed. The identical masses of the two ligands prevented further analysis of this library by ESI-MS. Although we cannot rule out the assembly of some quantity of a heteroleptic species $Fe_4L^E{}_4L^C{}_2$, these results allow us to infer that the pyrene-NDI π-stacking interactions in Fe-**5** are crucial to the clean assembly of the mixed-ligand assembly.

CONCLUSIONS

In conclusion, we have shown that the geometries of two isomeric bis(3-aminophenyl)pyrene derivatives enabled the construction of two unique metal–organic structure types, a C_2-symmetric rhomboidal $M^{II}{}_4L_6$ assembly with *mer* metal stereochemistry, and a C_3-symmetric self-included $M^{II}{}_4L_6$ pseudotetrahedron with *fac* coordination. Both structures are stabilized by π-stacking interactions, which were not present in $M^{II}{}_4L_6$ tetrahedral cages formed from their bis(4-aminophenyl)-pyrene congeners, demonstrating that small differences in subcomponent structure can result in incommensurate differences in the outcome of self-assembly processes. A lower-nuclearity $M^{II}{}_2L_2$ assembly was also obtained with one of the ligands, which was found to bind a range of electron-poor aromatics between two parallel pyrene units. This observation inspired the self-assembly of a unique $M^{II}{}_4L_4L'_2$ assembly featuring pyrene–pyrene–NDI triple stacks, the formation of which could be used to induce guest ejection from its $M^{II}{}_2L_2$ precursor. The $M^{II}{}_4L_4L'_2$ heteroleptic assembly was thermodynamically favored over the corresponding homoleptic $M^{II}{}_4L_6$ assemblies due to a combination of favorable π-stacking interactions, geometric and solvophobic effects. A deeper understanding of how secondary supramolecular interactions, such as π-stacking, can be combined with primary metal–ligand interactions may lead to the design of yet more complex and functional supramolecular architectures.

EXPERIMENTAL METHODS

General Methods. Unless otherwise specified, all starting materials were purchased from commercial sources and used as supplied. NMR spectra were recorded on a Bruker DRX-400, Bruker Avance 500 Cryo and a Bruker 500 TCI-ATM Cryo. ^{1}H Chemical shifts (δ) are reported in parts per million (ppm) and are reported relative to the solvent residual peaks. Low-resolution electrospray ionization mass spectra (ESI-MS) were obtained on a Micromass Quattro LC and high-resolution mass spectra acquired using a Thermofisher LTQ Orbitrap XL.

Synthesis of Zn-1. Zinc(II) triflimide (54 mg, 0.086 mmol), 1,6-bis(3-aminophenyl)pyrene (**A**, 50 mg, 0.130 mmol) and 2-formylpyridine (25 μL, 0.24 mmol) were dissolved in acetonitrile (25 mL). The reaction mixture was stirred under nitrogen at 323 K for 24 h. The volume was reduced to 10 mL in vacuo. The solution was layered with diethyl ether (30 mL) and kept at −4 °C for 24 h. The yellow microcrystalline solid was filtered and washed with excess diethyl ether. Yield 98 mg, 77%. ^{1}H NMR (500 MHz; 298 K; CD_3CN): δ 9.66 (s, 2H), 9.12 (d, 2H), 9.00 (s, 2H), 8.91 (s, 2H), 8.68 (s, 2H), 8.66 (d, 2H), 8.56 (m, 2H), 8.51 (m, 2H), 8.51 (m, 2H), 8.47 (m, 2H), 8.45 (m, 2H), 8.44 (m, 4H), 8.43 (m, 2H), 8.42 (m, 2H), 8.40 (m, 2H), 8.37 (m, 2H), 8.31 (m, 4H), 8.28 (m, 2H), 8.22 (d, 2H), 8.16 (m, 2H), 8.15 (m, 2H), 8.10 (d, 2H), 8.04 (d, 2H), 8.00 (m,

DOI: 10.1021/jacs.5b09920
J. Am. Chem. Soc. 2015, 137, 14502–14512

2H), 7.99 (m, 2H), 7.98 (m, 2H), 7.96 (m, 2H), 7.88 (m, 2H), 7.87 (m, 2H), 7.84 (m, 2H), 7.84 (m, 2H), 7.82 (m, 2H), 7.76 (m, 2H), 7.69 (m, 2H), 7.66 (t, 2H), 7.63 (m, 2H), 7.61 (m, 2H), 7.52 (m, 2H), 7.48 (m, 2H), 7.47 (m, 2H), 7.44 (m, 2H), 7.43 (m, 2H), 7.42 (m, 2H), 7.40 (m, 2H), 7.36 (m, 2H), 7.30 (m, 4H), 7.24 (m, 2H), 7.24 (m, 2H), 7.01 (m, 2H), 7.00 (m, 2H), 6.93 (m, 2H), 6.90 (m, 2H), 6.83 (m, 2H), 6.82 (m, 4H), 6.73 (d, 2H), 6.69 (d, 2H), 6.57 (s, 2H), 6.51 (d, 2H), 6.35 (m, 4H), 6.31 (d, 2H), 6.26 (s, 2H), 6.09 (d, 2H), 5.99 (d, 2H), 5.93 (d, 2H), 5.64 (d, 2H), 5.58 (d, 2H), 5.52 (d, 2H), 5.47 (t, 2H), 5.40 (s, 2H), 5.15 (d, 2H), 4.97 (s+d, 4H). ^{13}C NMR (126 MHz, 298 K, CD_3CN): δ = 163.8, 163.6, 163.0, 161.6, 160.8, 158.9, 150.9, 150.4, 150.1, 149.8, 148.5, 147.9, 147.4, 147.3, 147.2, 147.0, 146.8, 146.8, 146.3, 146.0, 145.9, 145.3, 145.0, 144.5, 144.5, 144.1, 143.8, 143.6, 143.5, 143.0, 142.9, 142.8, 142.7, 137.1, 136.9, 135.9, 135.8, 135.7, 134.2, 133.1, 132.9, 132.6, 132.1, 132.1, 131.9, 131.8, 131.6, 131.5, 131.4, 131.4, 131.3, 130.9, 130.8, 130.6, 130.6, 130.1, 129.7, 129.6, 129.5, 129.4, 129.3, 129.2, 129.2, 129.0, 128.8, 128.7, 128.3, 128.2, 128.0, 127.7, 127.5, 127.3, 127.0, 126.7, 126.7, 126.4, 126.2, 125.9, 125.8, 125.7, 125.6, 125.4, 125.2, 125.0, 124.7, 124.5, 124.1, 123.9, 122.1, 121.9, 121.4, 120.7, 120.6, 119.6, 119.2. ESI-MS: m/z = 454.6 [Zn-**1**]$^{8+}$, 559.9 [Zn-**1**(NTf_2^-)]$^{7+}$, 699.6 [Zn-**1**$(NTf_2^-)_2$]$^{6+}$, 895.4 [Zn-**1**$(NTf_2^-)_3$]$^{5+}$, 1189.5 [Zn-**1**$(NTf_2^-)_4$]$^{4+}$. Elemental Analysis (%) calcd for $C_{256}H_{156}F_{48}Zn_4N_{32}O_{32}S_{16}\cdot 10H_2O$: C, 50.75%; H, 2.93%; N, 7.40%. Found: C, 50.72%; H, 2.64%; N, 7.33%.

Synthesis of Co-1. Cobalt(II) triflimide (50 mg, 0.071 mmol), 1,6-bis(3-aminophenyl)pyrene (**A**, 40 mg, 0.104 mmol) and 2-formylpyridine (20 μL, 0.21 mmol) were dissolved in acetonitrile (25 mL). The reaction mixture was stirred under nitrogen at 323 K for 24 h. The volume was reduced to 10 mL in vacuo. The solution was layered with diethyl ether (30 mL) and kept at −4 °C for 24 h. The orange microcrystalline solid was filtered and washed with excess diethyl ether. Yield 66.5 mg, 66%. ^{1}H NMR (400 MHz; 298 K; CD_3CN): δ 272.99, 267.95, 254.07, 248.92, 217.01, 205.58, 183.77, 133.49, 132.22, 82.24, 80.90, 79.31, 75.30, 72.53, 70.25, 69.50, 62.23, 57.03, 50.24, 47.03, 31.61, 30.05, 28.56, 27.07, 26.74, 24.70, 21.16, 18.97, 16.76, 16.62, 14.45, 14.31, 12.58, 10.96, 10.86, 9.67, 9.18, 8.22, 8.05, 6.46, 6.29, 5.17, 3.64, 3.32, 2.99, 2.62, 1.48, 1.30, 1.19, 0.82, −0.15, −1.12, −1.88, −2.17, −2.61, −3.41, −3.84, −5.92, −8.37, −8.55, −10.04, −11.50, −12.53, −17.40, −17.62, −22.95, −35.84. ESI-MS: m/z = 451.1 [Co-**1**]$^{8+}$, 555.8 [Co-**1**(NTf_2^-)]$^{7+}$, 695.2 [Co-**1**$(NTf_2^-)_2$]$^{6+}$, 890.2 [Co-**1**$(NTf_2^-)_3$]$^{5+}$, 1182.9 [Co-**1**$(NTf_2^-)_4$]$^{4+}$. Elemental Analysis (%) calcd for $C_{256}H_{156}F_{48}Co_4N_{32}O_{32}S_{16}\cdot 8H_2O$: C, 51.27%; H, 2.89%; N, 7.47%. Found: C, 51.35%; H, 2.81%; N, 7.31%.

Synthesis of Zn-2. Zinc(II) triflimide (54 mg, 0.086 mmol), 2,7-bis(3-aminophenyl)pyrene (**B**, 50 mg, 0.130 mmol) and 2-formylpyridine (25 μL, 0.24 mmol) were dissolved in acetonitrile (25 mL). The reaction mixture was stirred under nitrogen at 323 K for 24 h. The volume was reduced to 10 mL in vacuo. The solution was layered with diethyl ether (30 mL) and kept at −4 °C for 24 h. The yellow microcrystalline solid was filtered and washed with excess diethyl ether. Yield 106 mg, 83%. ^{1}H NMR (500 MHz; 298 K; CD_3CN): δ9.22 (s, 3H, imine), 9.01 (s, 3H, imine), 8.77 (s, 3H, imine), 8.65 (td, 3H, pyridyl), 8.59 (s, 3H, imine), 8.58 (m, 3H, pyridyl), 8.50 (d, 3H, pyridyl), 8.47 (d, 3H, pyridyl), 8.38 (m, 3H, pyridyl), 8.37 (m, 3H, pyridyl), 8.36 (m, 3H, pyrene), 8.30 (m, 3H, pyridyl), 8.28 (m, 6H, 2× pyridyl), 8.18 (m, 3H, phenyl), 8.11 (m, 3H, phenyl), 8.08 (m, 3H, pyridyl), 8.02 (m, 3H, pyridyl), 7.99−8.02 (m, 6H, 2× pyridyl), 7.98 (m, 3H, pyridyl), 7.92 (m, 6H, pyridyl, phenyl), 7.91 (m, 3H, pyrene), 7.82 (m, 3H, phenyl), 7.79 (m, 3H, pyridyl), 7.78 (m, 3H, pyridyl), 7.75 (m, 3H, phenyl), 7.71 (d, 3H, phenyl), 7.69 (d, 3H, pyrene), 7.59 (d, 3H, phenyl), 7.32 (d, 3H, phenyl), 7.04 (dd, 3H, phenyl), 6.93 (t, 3H, phenyl), 6.50 (dd, 3H, phenyl), 6.44 (s, 3H, phenyl), 6.34 (d, 3H, pyrene), 6.24 (dd, 3H, phenyl), 6.22 (dd, 3H, phenyl), 6.00 (t, 3H, phenyl), 5.91 (t, 3H, phenyl), 5.88 (s, 3H, pyrene), 5.09 (s, 3H, pyrene), 4.12 (d, 3H, pyrene), 2.13 (d, 3H, pyrene). ^{13}C NMR (126 MHz, 298 K, CD_3CN): δ = 166.7, 166.5, 166.3, 166.2, 151.2, 150.9, 150.8, 149.9, 149.8, 149.7, 149.5, 149.1, 147.6, 147.6, 147.5, 146.8, 144.0, 144.0, 143.7, 143.1, 143.0, 142.4, 142.3, 136.6, 136.5, 134.7, 134.7, 133.0, 132.3, 132.3, 132.0, 131.9, 131.8, 131.4, 131.2, 131.0, 131.0, 130.7, 130.6, 130.1, 129.8, 129.4, 129.3, 128.5, 128.2, 128.0, 127.9, 127.6, 126.7, 126.5, 124.7, 124.6, 123.9, 123.3, 122.9, 122.8, 122.6, 122.6, 122.2, 121.9, 121.4, 121.2, 120.9, 120.6, 120.5, 120.4, 119.8, 119.6, 118.9. ESI-MS: m/z = 454.7 [Zn-**2**]$^{8+}$, 559.7 [Zn-**2**(NTf_2^-)]$^{7+}$, 699.6 [Zn-**2**$(NTf_2^-)_2$]$^{6+}$, 895.7 [Zn-**2**$(NTf_2^-)_3$]$^{5+}$, 1189.6 [Zn-**2**$(NTf_2^-)_4$]$^{4+}$. Elemental Analysis (%) calcd for $C_{256}H_{156}F_{48}Zn_4N_{32}O_{32}S_{16}\cdot 15H_2O$: C, 50.00%; H, 3.05%; N, 7.15%. Found: C, 49.98%; H, 2.69%; N, 7.15%.

Synthesis of Fe-2. Iron(II) triflimide (61.5 mg, 0.087 mmol), 2,7-bis(3-aminophenyl)pyrene (**B**, 50 mg, 0.130 mmol) and 2-formylpyridine (25 μL, 0.24 mmol) were dissolved in acetonitrile (25 mL). The reaction mixture was stirred under nitrogen at 353 K for 24 h. The volume was reduced to 10 mL in vacuo. The solution was layered with diethyl ether (30 mL) and kept at −4 °C for 24 h. The deep purple microcrystalline solid was filtered and washed with excess diethyl ether. Yield 119 mg, 94%. ^{1}H NMR (500 MHz; 298 K; CD_3CN): δ 9.70 (s, 3H, imine), 9.17 (s, 3H, imine), 9.06 (s, 3H, imine), 9.02 (s, 3H, imine), 8.73 (d, 3H, pyridyl), 8.70 (d, 3H, pyridyl), 8.64 (d, 3H, pyridyl), 8.60 (d, 3H, pyridyl), 8.55 (m, 3H, pyridyl), 8.54 (m, 3H, pyridyl), 8.46 (t, 3H, pyridyl), 8.31 (d, 3H, pyrene), 8.21 (d, 3H, phenyl), 8.15 (s, 3H, pyrene), 8.13 (m, 3H, pyridyl), 8.07 (t, 3H, phenyl), 7.99 (d, 3H, pyrene), 7.97 (d, 3H, pyrene), 7.92 (m, 3H, pyridyl), 7.91 (m, 3H, pyridyl), 7.88 (m, 3H, pyrene), 7.85 (m, 3H, phenyl), 7.78 (m, 3H, pyridyl), 7.78 (m, 3H, phenyl), 7.75 (m, 3H, phenyl), 7.72 (m, 3H, phenyl), 7.64 (s, 3H, pyrene), 7.62 (m, 3H, pyridyl), 7.59 (m, 3H, phenyl), 7.57 (m, 3H, pyrene), 7.55 (m, 3H, pyridyl), 7.54 (m, 3H, pyridyl), 7.46 (d, 3H, pyridyl), 7.26 (d, 3H, pyridyl), 7.17 (s, 3H, pyrene), 7.01 (d, 3H, phenyl), 6.82 (d, 3H, pyrene), 6.66 (s, 3H, pyrene), 6.53 (d, 3H, phenyl), 6.26 (s, 3H, pyrene), 6.20 (s, 3H, phenyl), 6.02 (d, 3H, phenyl), 5.85 (d, 3H, phenyl), 5.78 (s, 3H, pyrene), 5.77 (m, 3H, phenyl), 5.75 (s, 3H, phenyl), 5.70 (s, 3H, phenyl), 5.64 (d, 3H, pyrene), 5.58 (s, 3H, phenyl), 5.01 (s, 3H, pyrene), 4.21 (d, 3H, pyrene), 2.17 (d, 3H, pyrene). ^{13}C NMR (126 MHz, 298 K, CD_3CN): δ = 176.9, 176.8, 175.8, 175.7, 159.5, 159.3, 159.1, 158.9, 157.6, 157.5, 156.8, 155.7, 154.5, 152.5, 152.3, 151.7, 143.4, 143.3, 142.7, 142.5, 141.1, 140.9, 140.8, 136.8, 136.4, 134.6, 133.1, 132.8, 132.2, 132.0, 131.8, 131.7, 131.7, 131.3, 131.2, 131.2, 130.8, 130.8, 130.8, 130.6, 130.1, 129.9, 129.7, 129.4, 128.6, 128.4, 128.3, 127.4, 127.3, 127.0, 126.3, 125.1, 124.7, 124.5, 124.0, 123.7, 123.3, 123.2, 123.2, 123.1, 122.8, 122.4, 122.3, 122.7, 121.8, 121.5, 121.2, 120.6, 120.5, 120.3, 120.1, 119.6. ESI-MS: m/z = 449.9 [Fe-**2**]$^{8+}$, 554.3 [Fe-**2**(NTf_2^-)]$^{7+}$, 693.4 [Fe-**2**$(NTf_2^-)_2$]$^{6+}$, 888.0 [Fe-**2**$(NTf_2^-)_3$]$^{5+}$, 1180.0 [Fe-**2**$(NTf_2^-)_4$]$^{4+}$. Elemental Analysis (%) calcd for $C_{256}H_{156}F_{48}Fe_4N_{32}O_{32}S_{16}\cdot 11H_2O$: C, 50.92%; H, 2.97%; N, 7.42%. Found: C, 50.97%; H, 2.79%; N, 7.21%.

Synthesis of Co-2. Cobalt(II) triflimide (36.8 mg, 0.052 mmol), 2,7-bis(3-aminophenyl)pyrene (**B**, 30 mg, 0.078 mmol) and 2-formylpyridine (15 μL, 0.16 mmol) were dissolved in acetonitrile (15 mL). The reaction mixture was stirred under nitrogen at 353 K for 24 h. The volume was reduced to 5 mL in vacuo. The solution was layered with diethyl ether (20 mL) and kept at −4 °C for 24 h. The orange microcrystalline solid was filtered and washed with excess diethyl ether. Yield 56 mg, 74%. ^{1}H NMR (400 MHz; 298 K; CD_3CN): δ 250.17, 247.14, 241.84, 233.86, 126.68, 86.42, 82.06, 75.77, 73.95, 72.49, 71.79, 60.26, 57.91, 52.18, 49.79, 49.54, 18.06, 16.33, 15.13, 14.62, 13.53, 11.66, 10.02, 9.85, 8.80, 8.79, 7.96, 7.94, 7.61, 5.45, 2.62, 1.27, −2.19, −2.21, −2.54, −6.80, −7.69, −7.71, −8.25, −8.26, −10.68, −12.06, −12.92, −13.67, −13.70, −21.47, −21.63, −26.10, −28.61, −33.39, −56.52, −81.35. ESI-MS: m/z = 451.5 [Co-**2**]$^{8+}$, 556.0 [Co-**2**(NTf_2^-)]$^{7+}$, 695.4 [Co-**2**$(NTf_2^-)_2$]$^{6+}$, 890.5 [Co-**2**$(NTf_2^-)_3$]$^{5+}$, 1183.1 [Co-**2**$(NTf_2^-)_4$]$^{4+}$. Elemental Analysis (%) calcd for $C_{256}H_{156}F_{48}Co_4N_{32}O_{32}S_{16}\cdot 13H_2O$: C, 50.51%; H, 3.01%; N, 7.36%. Found: C, 50.35%; H, 2.67%; N, 7.17%.

Synthesis of Zn-3. Zinc(II) triflimide (49 mg, 0.078 mmol), 2,7-bis(3-aminophenyl)pyrene (**B**, 30 mg, 0.078 mmol) and 2-formylpyridine (15 μL, 0.16 mmol) were dissolved in acetonitrile (5 mL). The reaction mixture was stirred under nitrogen at 323 K for 24 h. The volume was reduced to 3 mL in vacuo. The solution was

DOI: 10.1021/jacs.5b09920
J. Am. Chem. Soc. 2015, 137, 14502−14512

layered with diethyl ether (10 mL) and kept at −4 °C for 24 h. The yellow-orange microcrystalline solid was filtered and washed with excess diethyl ether. Yield 75 mg, 81%. ^{1}H NMR (400 MHz; 298 K; CD_3CN): δ 8.93 (s, 4H, imine), 8.80 (d, J = 4.0 Hz, 4H, pyridyl), 8.46 (t, J = 7.7 Hz, 4H, pyridyl), 8.21 (d, J = 7.7 Hz, 4H, pyridyl), 8.04 (m, 4H, pyridyl), 7.94 (s, 8H, pyrene), 7.79 (d, J = 7.6 Hz, 4H, phenyl), 7.54 (s, 8H, pyrene), 7.47 (t, J = 7.8 Hz, 4H, phenyl), 7.39 (s, 4H, phenyl), 6.95 (d, J = 7.7 Hz, 4H, phenyl). ^{13}C NMR (126 MHz, 298 K, CD_3CN): δ = 163.5 (imine), 150.5, 147.9, 147.4, 143.8, 143.5, 137.6, 132.0, 131.1, 131.1, 131.0, 128.9, 128.2, 124.0, 123.7, 122.2, 121.2, 119.6. ESI-MS: m/z = 334.4 [Zn-**3**$(MeCN)_2]^{4+}$, 525.4 [Zn-**3**$(MeCN)(NTf_2^-)]^{3+}$, 908.1 [Zn-**3**$(NTf_2^-)_2]^{2+}$. Elemental Analysis (%) calcd for $Zn_2C_{88}H_{52}F_{24}N_{12}O_{16}S_8$: C, 44.52%; H, 2.21%; N, 7.08%. Found: C, 44.88%; H, 2.49%; N, 6.70%.

Synthesis of Co-3. Cobalt(II) triflimide (18.4 mg, 0.026 mmol), 2,7-bis(3-aminophenyl)pyrene (**B**, 10 mg, 0.026 mmol) and 2-formylpyridine (5.0 μL, 0.052 mmol) were dissolved in acetonitrile (2 mL). The reaction mixture was stirred under nitrogen at 323 K for 24 h. The volume was reduced to 1 mL in vacuo. The solution was layered with diethyl ether (3 mL) and kept at −4 °C for 24 h. The orange microcrystalline solid was filtered and washed with excess diethyl ether. Yield 25 mg, 81%. ^{1}H NMR (400 MHz; 298 K; CD_3CN): δ 273.5 (br), 83.1 (br), 56.8 (br), 21.2, −10.8 (br), −13.7 (br) [several peaks were overlapping or too broad to identify]. ESI-MS: m/z = 534.9 [Co-**3**$(MeCN)_2(NTf_2^-)]^{3+}$, 901.3 [Co-**3**$(NTf_2^-)_2]^{2+}$. Elemental Analysis (%) calcd for $Co_2C_{88}H_{52}F_{24}N_{12}O_{16}S_8$: C, 44.71%; H, 2.22%; N, 7.11%. Found: C, 44.74%; H, 2.46%; N, 7.02%.

Synthesis of Fe-4. NDI diamine **C** (224 mg, 0.5 mmol), iron(II) triflimide (235 mg, 0.332 mmol) and 2-formylpyridine (95 μL, 1 mmol) were added to a Schlenk flask along with acetonitrile (15 mL). The flask was sealed and purged of dioxygen by three vacuum/nitrogen fill cycles and sonicated for 0.5 h. The flask was heated at 323 K for 24 h. The crude product was purified from the starting material by filtration through Celite followed by precipitation with diethyl ether. Fe-**4** was obtained as a purple powder (401 mg, 78%). ^{1}H NMR (400 MHz: CD_3CN) δ = 9.12−8.98 (12H, m, imine), 8.76−8.51 (36H, m, NDI and pyridyl), 8.41 (12H, bs, pyridyl), 7.78 (12H, bs, pyridyl), 7.57−7.33 (36H, m, phenyl and pyridyl), 6.08−5.27 (24H, m, phenyl). ^{13}C NMR (125 MHz: CD_3CN) δ = 176.6, 176.1, 176.0, 164.4, 164.2, 164.1, 164.1, 164.0, 163.8, 159.0, 158.9, 159.9 156.8, 156.6, 151.3, 151.2, 150.7, 140.7, 140.6, 140.5, 136.7, 136.5, 136.4, 136.3, 132.4, 132.3, 132.2, 131.9, 131.5, 131.3, 130.7, 130.6 130.0, 128.2, 128.1, 128.0, 128.0, 124.6, 124.5, 123.2, 123.0, 122.9, 122.0, 120.0, 119.4, 116.8, 116.6, 116.3, 115.5. ESI-MS: m/z = 498.0 [Fe-**4**$]^{8+}$, 609.0 [Fe-**4**$(NTf_2^-)]^{7+}$, 757.1 [Fe-**4**$(NTf_2^-)_2]^{6+}$, 964.7 [Fe-**4**$(NTf_2^-)_3]^{5+}$, 1275.9 [Fe-**4**$(NTf_2^-)_4]^{4+}$. Elemental Analysis (%) calcd for $C_{244}H_{132}N_{44}O_{56}F_{48}S_{16}Fe_4{\cdot}7H_2O$: C 46.14, H 2.32, N 9.71. Found; C 46.17, H 2.34, N 9.65.

Synthesis of Co-4. NDI diamine **C** (168 mg, 0.374 mmol), Cobalt(II) triflimide (163 mg, 0.284 mmol) and 2-formylpyridine (71.2 μL, 0.748 mmol) were added to a Schlenk flask with 10 mL of acetonitrile. The flask was heated at 323 K for 24 h. The crude product was purified by filtration through a plug of Celite and precipitation with diethyl ether. Co-**4** was obtained as an orange crystalline solid (263 mg, 68%). ^{1}H NMR (400 MHz: $CD_3CN/CHCl_3$ 1:1) δ = 246.43, 243.26, 94.27, 88.03−88.95, 74.17, 72.70, 71.66, 52.53, 51.62, 51.32, 16.69, 16.17, 15.64, 7.55, −3.93, − 45.11, − 51.32, − 56.88. ESI-MS m/z: 499.5 [Co-**4**$]^{8+}$, 610.8 [Co-**4**$(NTf_2^-)]^{7+}$, 759.3 [Co-**4**$(NTf_2^-)_2]^{6+}$, 967.1 [Co-**4**$(NTf_2^-)_3]^{5+}$, 1278.9 [Co-**4**$(NTf_2^-)_4]^{4+}$.

Synthesis of Zn-5. Zinc(II) triflimide (24.4 mg, 0.039 mmol), 2,7-bis(3-aminophenyl)pyrene (**B**, 15 mg, 0.039 mmol), NDI diamine **C** (8.8 mg, 0.020 mmol) and 2-formylpyridine (11.3 μL, 0.12 mmol) were dissolved in acetonitrile (5 mL). The reaction mixture was stirred under nitrogen at 323 K for 24 h. The volume was reduced to 2 mL in vacuo. The solution was layered with diethyl ether (5 mL) and kept at −4 °C for 24 h. The organge microcrystalline solid was filtered and washed with excess diethyl ether. Yield 56 mg, 96%. ^{1}H NMR (500 MHz; 298 K; CD_3CN): δ 8.98 (s), 8.90 (s), 8.87 (s), 8.86 (s), 8.78−8.84 (m), 8.73 (s), 8.47−8.70 (m), 8.43 (d), 8.38 (d), 7.76−8.36 (m), 7.43−7.70 (m), 7.39 (d), 7.10 (m), 7.06 (m), 6.95 (d), 6.80 (s), 6.67 (d), 6.31 (d), 6.24 (d), 6.12 (dd), 6.09 (s), 6.01 (dd), 5.78 (s), 5.47 (s). ESI-MS: m/z = 470.2 [Zn-**5**$]^{8+}$, 720.8 [Zn-**5**$(NTf_2^-)_2]^{6+}$, 921.2 [Zn-**5**$(NTf_2^-)_3]^{5+}$, 1221.4 [Zn-**5**$(NTf_2^-)_4]^{4+}$. Elemental Analysis (%) calcd for $Zn_4C_{252}H_{148}F_{48}N_{36}O_{40}S_{16}{\cdot}6H_2O$: C, 49.50%; H, 2.64%; N, 8.25%. Found: C, 49.49%; H, 2.56%; N, 8.18%.

Synthesis of Co-5. Cobalt(II) triflimide (27.6 mg, 0.039 mmol), 2,7-bis(3-aminophenyl)pyrene (**B**, 15 mg, 0.039 mmol), NDI diamine C (8.8 mg, 0.020 mmol) and 2-formylpyridine (11.3 μL, 0.12 mmol) were dissolved in acetonitrile (5 mL). The reaction mixture was stirred under nitrogen at 353 K for 24 h. The volume was reduced to 2 mL in vacuo. The solution was layered with diethyl ether (5 mL) and kept at −4 °C for 24 h. The orange microcrystalline solid was filtered and washed with excess diethyl ether. Yield 49 mg, 84%. ^{1}H NMR (400 MHz; 298 K; CD_3CN): δ 256.00, 251.05, 249.09, 245.89, 245.68, 244.08, 230.54, 227.89, 136.71, 109.80, 94.48, 87.53, 79.95, 77.67, 75.36, 74.96, 74.27, 73.68, 73.48, 72.50, 67.20, 61.20, 57.55, 55.42, 52.95, 52.43, 52.03, 51.72, 50.95, 28.89, 28.07, 24.45, 21.80, 21.08, 18.75, 18.28, 17.02, 16.84, 16.32, 15.79, 15.50, 15.19, 14.44, 13.82, 13.11, 10.02, 9.02, 8.79, 7.95, 7.61, 5.45, 0.88, 0.75, 0.52, 0.44, 0.30, −0.40, −1.67, −1.87, −2.34, −3.58, −5.25, −6.83, −9.53, −13.42, −15.61, −15.73, −16.78, −17.26, −20.94, −22.50, −51.34, −55.16, −55.35, −61.19, −84.33. ESI-MS: m/z = 716.5 [Co-**5**$(NTf_2^-)_2]^{6+}$, 915.8 [Co-**5**$(NTf_2^-)_3]^{5+}$, 1214.8 [Co-**5**$(NTf_2^-)_4]^{4+}$. Elemental Analysis (%) calcd for $Co_4C_{252}H_{148}F_{48}N_{36}O_{40}S_{16}{\cdot}12H_2O$: C, 48.84%; H, 2.80%; N, 8.14%. Found: C, 48.73%; H, 2.57%; N, 8.20%.

Synthesis of Fe-5. Iron(II) triflimide (27.6 mg, 0.039 mmol), 2,7-bis(3-aminophenyl)pyrene (**B**, 15 mg, 0.039 mmol), NDI diamine **C** (8.8 mg, 0.020 mmol) and 2-formylpyridine (11.3 μL, 0.12 mmol) were dissolved in acetonitrile (5 mL). The reaction mixture was stirred under nitrogen at 353 K for 24 h. The volume was reduced to 2 mL in vacuo. The solution was layered with diethyl ether (5 mL) and kept at −4 °C for 24 h. The deep purple microcrystalline solid was filtered and washed with excess diethyl ether. Yield 52 mg, 89%. ^{1}H NMR (500 MHz; 298 K; CD_3CN): δ 9.33 (d), 9.18 (s), 9.12 (s), 9.06 (s), 9.03 (s), 8.99 (s), 8.97 (s), 8.87 (s), 8.28−8.78 (m), 8.10−8.21 (m), 7.30−7.95 (m), 7.14−7.19 (m), 7.02 (d), 6.98 (dd), 6.73 (m), 6.67 (m), 6.56 (td), 6.52 (d), 6.43 (d), 6.06 (dd), 5.98 (d), 5.92 (m), 5.89 (m), 5.82 (m), 5.76 (dd), 5.71 (dd), 5.60 (m), 5.56 (dd), 5.51 (dd), 5.28 (s), 5.10 (s). ESI-MS: m/z = 465.8 [Fe-**5**$]^{8+}$, 572.4 [Fe-**5**$(NTf_2^-)]^{7+}$, 714.4 [Fe-**5**$(NTf_2^-)_2]^{6+}$, 913.4 [Fe-**5**$(NTf_2^-)_3]^{5+}$, 1211.6 [Fe-**5**$(NTf_2^-)_4]^{4+}$. Elemental Analysis (%) calcd for $Fe_4C_{252}H_{148}F_{48}N_{36}O_{40}S_{16}{\cdot}11H_2O$: C, 49.08%; H, 2.78%; N, 8.18%. Found: C, 48.88%; H, 2.51%; N, 8.19%.

■ ASSOCIATED CONTENT

Supporting Information

The Supporting Information is available free of charge on the ACS Publications website at DOI: 10.1021/jacs.5b09920. Crystallographic data have been deposited with the Cambridge Crystallographic Data Centre as entries CCDC 1420852−1420858 and 1426149.

Synthetic procedures and characterization of subcomponents **A** and **B**, characterization of metal−organic assemblies, spectroscopic data, details of guest-binding and self-sorting investigations. (PDF)

Crystallographic data for Co-**1**. (CIF)

Crystallographic data for Co-**4**. (CIF)

Crystallographic data for Fe-**2**. (CIF)

Crystallographic data for Zn-**1**. (CIF)

Crystallographic data for TCNQ⊂Zn-**3**. (CIF)

Crystallographic data for Zn-**3**. (CIF)

Crystallographic data for Zn-**5**. (CIF)

Crystallographic data for Co-**3**. (CIF)

DOI: 10.1021/jacs.5b09920
J. Am. Chem. Soc. 2015, 137, 14502−14512

AUTHOR INFORMATION

Corresponding Author

*jrn34@cam.ac.uk

Notes

The authors declare no competing financial interest.

ACKNOWLEDGMENTS

This work was supported by the UK Engineering and Physical Sciences Research Council (EPSRC). D.A.R. acknowledges the Gates Cambridge Trust for Ph.D. funding (Gates Cambridge Scholarship). We thank the EPSRC Mass Spectrometry Service at Swansea for carrying out the high resolution mass spectrometry and Diamond Light Source (UK) for synchrotron beamtime on I19 (MT8464). We also thank the NMR service team at the Department of Chemistry, University of Cambridge for performing some of the NMR experiments.

REFERENCES

(1) (a) Mukherjee, S.; Mukherjee, P. S. *Chem. Commun.* **2014**, *50*, 2239. (b) Cook, T. R.; Stang, P. J. *Chem. Rev.* **2015**, *115*, 7001. (c) Han, M.; Engelhard, D. M.; Clever, G. H. *Chem. Soc. Rev.* **2014**, *43*, 1848. (d) Nakamura, T.; Ube, H.; Shionoya, M. *Chem. Lett.* **2013**, *42*, 328.

(2) (a) Wang, Q.-Q.; Day, V. W.; Bowman-James, K. *Angew. Chem., Int. Ed.* **2012**, *51*, 2119. (b) Whitehead, M.; Turega, S.; Stephenson, A.; Hunter, C. A.; Ward, M. D. *Chem. Sci.* **2013**, *4*, 2744. (c) Wang, J.; He, C.; Wu, P.; Wang, J.; Duan, C. *J. Am. Chem. Soc.* **2011**, *133*, 12402. (d) Fiedler, D.; Leung, D. H.; Bergman, R. G.; Raymond, K. N. *Acc. Chem. Res.* **2005**, *38*, 349. (e) Mishra, A.; Vajpayee, V.; Kim, H.; Lee, M. H.; Jung, H.; Wang, M.; Stang, P. J.; Chi, K.-W. *Dalton Trans.* **2012**, *41*, 1195.

(3) Riddell, I. A.; Smulders, M. M. J.; Clegg, J. K.; Nitschke, J. R. *Chem. Commun.* **2011**, *47*, 457.

(4) Breiner, B.; Clegg, J. K.; Nitschke, J. R. *Chem. Sci.* **2011**, *2*, 51.

(5) Brown, C. J.; Toste, F. D.; Bergman, R. G.; Raymond, K. N. *Chem. Rev.* **2015**, *115*, 3012.

(6) Caulder, D. L.; Raymond, K. N. *J. Chem. Soc., Dalton Trans.* **1999**, 1185.

(7) Zhou, X.-P.; Liu, J.; Zhan, S.-Z.; Yang, J.-R.; Li, D.; Ng, K.-M.; Sun, R. W.-Y.; Che, C.-M. *J. Am. Chem. Soc.* **2012**, *134*, 8042.

(8) (a) Kaifer, A. E.; Yi, S.; Brega, V.; Captain, B. *Chem. Commun.* **2012**, *48*, 10295. (b) Mahata, K.; Frischmann, P. D.; Würthner, F. *J. Am. Chem. Soc.* **2013**, *135*, 15656.

(9) (a) Tidmarsh, I. S.; Faust, T. B.; Adams, H.; Harding, L. P.; Russo, L.; Clegg, W.; Ward, M. D. *J. Am. Chem. Soc.* **2008**, *130*, 15167. (b) Ramsay, W. J.; Szczypiński, F. T.; Weissman, H.; Ronson, T. K.; Smulders, M. M. J.; Rybtchinski, B.; Nitschke, J. R. *Angew. Chem., Int. Ed.* **2015**, *54*, 5636.

(10) Ronson, T. K.; Fisher, J.; Harding, L. P.; Hardie, M. J. *Angew. Chem., Int. Ed.* **2007**, *46*, 9086.

(11) Pasquale, S.; Sattin, S.; Escudero-Adán, E. C.; Martínez-Belmonte, M.; de Mendoza, J. *Nat. Commun.* **2012**, *3*, 785.

(12) (a) Harris, K.; Fujita, D.; Fujita, M. *Chem. Commun.* **2013**, *49*, 6703. (b) Gütz, C.; Hovorka, R.; Klein, C.; Jiang, Q.-Q.; Bannwarth, C.; Engeser, M.; Schmuck, C.; Assenmacher, W.; Mader, W.; Topić, F.; Rissanen, K.; Grimme, S.; Lützen, A. *Angew. Chem., Int. Ed.* **2014**, *53*, 1693.

(13) (a) Engelhard, D. M.; Freye, S.; Grohe, K.; John, M.; Clever, G. H. *Angew. Chem., Int. Ed.* **2012**, *51*, 4747. (b) Ward, M. D. *Chem. Commun.* **2009**, 4487. (c) Saalfrank, R. W.; Maid, H.; Scheurer, A. *Angew. Chem., Int. Ed.* **2008**, *47*, 8794.

(14) He, Z.; Jiang, W.; Schalley, C. A. *Chem. Soc. Rev.* **2015**, *44*, 779.

(15) Smulders, M. M. J.; Riddell, I. A.; Browne, C.; Nitschke, J. R. *Chem. Soc. Rev.* **2013**, *42*, 1728.

(16) (a) Saha, M. L.; Schmittel, M. *J. Am. Chem. Soc.* **2013**, *135*, 17743. (b) Mahata, K.; Schmittel, M. *J. Am. Chem. Soc.* **2009**, *131*, 16544.

(17) De, S.; Mahata, K.; Schmittel, M. *Chem. Soc. Rev.* **2010**, *39*, 1555.

(18) (a) Mirtschin, S.; Slabon-Turski, A.; Scopelliti, R.; Velders, A. H.; Severin, K. *J. Am. Chem. Soc.* **2010**, *132*, 14004. (b) Jayamurugan, G.; Roberts, D. A.; Ronson, T. K.; Nitschke, J. R. *Angew. Chem., Int. Ed.* **2015**, *54*, 7539. (c) Zhao, Z.; Zheng, Y.-R.; Wang, M.; Pollock, J. B.; Stang, P. J. *Inorg. Chem.* **2010**, *49*, 8653. (d) Ye, Y.; Cook, T. R.; Wang, S. P.; Wu, J.; Li, S.; Stang, P. J. *J. Am. Chem. Soc.* **2015**, *137*, 11896. (e) Shi, Y.; Sanchez-Molina, I.; Cao, C.; Cook, T. R.; Stang, P. J. *Proc. Natl. Acad. Sci. U. S. A.* **2014**, *111*, 9390.

(19) (a) Yamashina, M.; Yuki, T.; Sei, Y.; Akita, M.; Yoshizawa, M. *Chem. - Eur. J.* **2015**, *21*, 4200. (b) Sun, Q.-F.; Sato, S.; Fujita, M. *Angew. Chem., Int. Ed.* **2014**, *53*, 13510. (c) Argent, S. P.; Adams, H.; Riis-Johannessen, T.; Jeffery, J. C.; Harding, L. P.; Ward, M. D. *J. Am. Chem. Soc.* **2006**, *128*, 72. (d) Wood, C. S.; Ronson, T. K.; Belenguer, A. M.; Holstein, J. J.; Nitschke, J. R. *Nat. Chem.* **2015**, *7*, 354. (e) Schultz, A.; Li, X.; Barkakaty, B.; Moorefield, C. N.; Wesdemiotis, C.; Newkome, G. R. *J. Am. Chem. Soc.* **2012**, *134*, 7672. (f) Samanta, D.; Mukherjee, P. S. *Chem. Commun.* **2013**, *49*, 4307. (g) Yan, L.-L.; Tan, C.-H.; Zhang, G.-L.; Zhou, L.-P.; Bünzli, J.-C.; Sun, Q.-F. *J. Am. Chem. Soc.* **2015**, *137*, 8550.

(20) Northrop, B. H.; Zheng, Y.-R.; Chi, K.-W.; Stang, P. J. *Acc. Chem. Res.* **2009**, *42*, 1554.

(21) Johnson, A. M.; Hooley, R. J. *Inorg. Chem.* **2011**, *50*, 4671.

(22) (a) Riddell, I. A.; Hristova, Y. R.; Clegg, J. K.; Wood, C. S.; Breiner, B.; Nitschke, J. R. *J. Am. Chem. Soc.* **2013**, *135*, 2723. (b) Giles, I. D.; Chifotides, H. T.; Shatruk, M.; Dunbar, K. R. *Chem. Commun.* **2011**, *47*, 12604. (c) Custelcean, R.; Bonnesen, P. V.; Duncan, N. C.; Zhang, X.; Watson, L. A.; Van Berkel, G.; Parson, W. B.; Hay, B. P. *J. Am. Chem. Soc.* **2012**, *134*, 8525. (d) Klein, C.; Gütz, C.; Bogner, M.; Topić, F.; Rissanen, K.; Lützen, A. *Angew. Chem., Int. Ed.* **2014**, *53*, 3739.

(23) (a) Wood, D. M.; Meng, W.; Ronson, T. K.; Stefankiewicz, A. R.; Sanders, J. K. M.; Nitschke, J. R. *Angew. Chem., Int. Ed.* **2015**, *54*, 3988. (b) Bilbeisi, R. A.; Clegg, J. K.; Elgrishi, N.; de Hatten, X.; Devillard, M.; Breiner, B.; Mal, P.; Nitschke, J. R. *J. Am. Chem. Soc.* **2012**, *134*, 5110.

(24) (a) Gabriel, G. J.; Iverson, B. L. *J. Am. Chem. Soc.* **2002**, *124*, 15174. (b) Zhu, Z.; Bruns, C. J.; Li, H.; Lei, J.; Ke, C.; Liu, Z.; Shafaie, S.; Colquhoun, H. M.; Stoddart, J. F. *Chem. Sci.* **2013**, *4*, 1470.

(25) (a) Basu, S.; Coskun, A.; Friedman, D. C.; Olson, M. A.; Benítez, D.; Tkatchouk, E.; Barin, G.; Yang, J.; Fahrenbach, A. C.; Goddard, W. A.; Stoddart, J. F. *Chem. - Eur. J.* **2011**, *17*, 2107. (b) Bruns, C. J.; Li, J.; Frasconi, M.; Schneebeli, S. T.; Iehl, J.; Jacquot de Rouville, H.-P.; Stupp, S. I.; Voth, G. A.; Stoddart, J. F. *Angew. Chem., Int. Ed.* **2014**, *53*, 1953. (c) Hansen, S. W.; Stein, P. C.; Sørensen, A.; Share, A. I.; Witlicki, E. H.; Kongsted, J.; Flood, A. H.; Jeppesen, J. O. *J. Am. Chem. Soc.* **2012**, *134*, 3857.

(26) (a) Cougnon, F. B. L.; Au-Yeung, H. Y.; Pantoş, G. D.; Sanders, J. K. M. *J. Am. Chem. Soc.* **2011**, *133*, 3198. (b) Zhu, Z.; Fahrenbach, A. C.; Li, H.; Barnes, J. C.; Liu, Z.; Dyar, S. M.; Zhang, H.; Lei, J.; Carmieli, R.; Sarjeant, A. A.; Stern, C. L.; Wasielewski, M. R.; Stoddart, J. F. *J. Am. Chem. Soc.* **2012**, *134*, 11709.

(27) (a) Yoshizawa, M.; Nakagawa, J.; Kurnazawa, K.; Nagao, M.; Kawano, M.; Ozeki, T.; Fujita, M. *Angew. Chem., Int. Ed.* **2005**, *44*, 1810. (b) Yamauchi, Y.; Yoshizawa, M.; Akita, M.; Fujita, M. *J. Am. Chem. Soc.* **2010**, *132*, 960.

(28) Baram, J.; Weissman, H.; Tidhar, Y.; Pinkas, I.; Rybtchinski, B. *Angew. Chem., Int. Ed.* **2014**, *53*, 4123.

(29) Black, S. P.; Stefankiewicz, A. R.; Smulders, M. M. J.; Sattler, D.; Schalley, C. A.; Nitschke, J. R.; Sanders, J. K. M. *Angew. Chem., Int. Ed.* **2013**, *52*, 5749.

(30) Wang, J.; Wang, M.; Xiang, J.; Cao, L.; Wu, A.; Isaacs, L. *CrystEngComm* **2015**, *17*, 2486.

(31) (a) Ronson, T. K.; Zarra, S.; Black, S. P.; Nitschke, J. R. *Chem. Commun.* **2013**, *49*, 2476. (b) Sham, K.-C.; Yiu, S.-M.; Kwong, H.-L. *Inorg. Chem.* **2013**, *52*, 5648. (c) Lewing, D.; Koppetz, H.; Hahn, F. E. *Inorg. Chem.* **2015**, *54*, 7653. (d) Gorczynski, A.; Kubicki, M.; Pinkowicz, D.; Pelka, R.; Patroniak, V.; Podgajny, R. *Dalton Trans.*

DOI: 10.1021/jacs.5b09920
J. Am. Chem. Soc. 2015, 137, 14502−14512

2015, *44*, 16833. (e) Frischmann, P. D.; Kunz, V.; Würthner, F. *Angew. Chem., Int. Ed.* **2015**, *54*, 7285. (f) Ren, D.-H.; Qiu, D.; Pang, C.-Y.; Li, Z.; Gu, Z.-G. *Chem. Commun.* **2015**, *51*, 788. (g) Bunzen, H.; Nonappa; Kalenius, E.; Hietala, S.; Kolehmainen, E. *Chem. - Eur. J.* **2013**, *19*, 12978. (h) Yi, S.; Brega, V.; Captain, B.; Kaifer, A. E. *Chem. Commun.* **2012**, *48*, 10295.

(32) Ronson, T. K.; League, A. B.; Gagliardi, L.; Cramer, C. J.; Nitschke, J. R. *J. Am. Chem. Soc.* **2014**, *136*, 15615.

(33) Miyaura, N.; Suzuki, A. *Chem. Rev.* **1995**, *95*, 2457.

(34) Foroozandeh, M.; Adams, R. W.; Meharry, N. J.; Jeannerat, D.; Nilsson, M.; Morris, G. A. *Angew. Chem., Int. Ed.* **2014**, *53*, 6990.

(35) (a) Paul, R. L.; Argent, S. P.; Jeffery, J. C.; Harding, L. P.; Lynam, J. M.; Ward, M. D. *Dalton Trans.* **2004**, 3453. (b) Young, M. C.; Holloway, L. R.; Johnson, A. M.; Hooley, R. J. *Angew. Chem., Int. Ed.* **2014**, *53*, 9832.

(36) (a) Browne, C.; Ramsay, W. J.; Ronson, T. K.; Medley-Hallam, J.; Nitschke, J. R. *Angew. Chem., Int. Ed.* **2015**, *54*, 11122. (b) Hall, B. R.; Adams, H.; Ward, M. D. *Supramol. Chem.* **2012**, *24*, 499.

(37) Ronson, T. K.; Nelson, J.; Jameson, G. B.; Jeffery, J. C.; Brooker, S. *Eur. J. Inorg. Chem.* **2004**, *2004*, 2570.

(38) Beissel, T.; Powers, R. E.; Parac, T. N.; Raymond, K. N. *J. Am. Chem. Soc.* **1999**, *121*, 4200.

(39) (a) Davis, A. V.; Raymond, K. N. *J. Am. Chem. Soc.* **2005**, *127*, 7912. (b) Davis, A. V.; Fiedler, D.; Seeber, G.; Zahl, A.; Van Eldik, R.; Raymond, K. N. *J. Am. Chem. Soc.* **2006**, *128*, 1324.

(40) (a) Frank, M.; Krause, L.; Herbst-Irmer, R.; Stalke, D.; Clever, G. H. *Dalton Trans.* **2014**, *43*, 4587. (b) Osowska, K.; Miljanić, O. Š. *J. Am. Chem. Soc.* **2011**, *133*, 724. (c) Zheng, Y.-R.; Yang, H.-B.; Northrop, B. H.; Ghosh, K.; Stang, P. J. *Inorg. Chem.* **2008**, *47*, 4706.

(41) Xu, J.; Parac, T. N.; Raymond, K. N. *Angew. Chem., Int. Ed.* **1999**, *38*, 2878.

(42) Dobrowolski, M. A.; Garbarino, G.; Mezouar, M.; Ciesielski, A.; Cyranski, M. K. *CrystEngComm* **2014**, *16*, 415.

(43) (a) Fang, L.; Basu, S.; Sue, C.-H.; Fahrenbach, A. C.; Stoddart, J. F. *J. Am. Chem. Soc.* **2011**, *133*, 396. (b) Cougnon, F. B. L.; Ponnuswamy, N.; Jenkins, N. A.; Pantoş, G. D.; Sanders, J. K. M. *J. Am. Chem. Soc.* **2012**, *134*, 19129.

(44) Black, S. P.; Wood, D. M.; Schwarz, F. B.; Ronson, T. K.; Holstein, J. J.; Stefankiewicz, A. R.; Schalley, C. A.; Sanders, J. K. M.; Nitschke, J. R., submitted manuscript.

(45) Cubberley, M. S.; Iverson, B. L. *J. Am. Chem. Soc.* **2001**, *123*, 7560.

(46) (a) Jiang, W.; Winkler, H. D. F.; Schalley, C. A. *J. Am. Chem. Soc.* **2008**, *130*, 13852. (b) Safont-Sempere, M. M.; Fernández, G.; Würthner, F. *Chem. Rev.* **2011**, *111*, 5784.

(47) Preliminary self-assembly experiments with diamine **E** and zinc(II) indicate that a mixture of assemblies is obtained including M_4L_6 and M_2L_3 assemblies.

DOI: 10.1021/jacs.5b09920
J. Am. Chem. Soc. 2015, 137, 14502−14512